

# Determination of Electronic Structure of Oxide–Oxide Interfaces by Photoemission Spectroscopy

By Hui-Qiong Wang, Eric Altman, Christine Broadbridge, Yimei Zhu, and Victor Henrich\*

A method has been developed to use the finite escape depth of the photoelectrons emitted in ultraviolet photoemission spectroscopy (UPS) to determine the electronic density-of-states at the interface between two dissimilar metal oxides. Ultrathin films of one oxide are grown heteroepitaxially, one monolayer at a time, on a single-crystal substrate of the other oxide, and UPS spectra are taken after each complete monolayer. By comparing experimental UPS spectra with calculated spectra based on specific models of the interfacial structure, the interfacial density-of-states can be extracted. The two oxide systems studied here are NiO–Fe<sub>3</sub>O<sub>4</sub> and CoO–Fe<sub>3</sub>O<sub>4</sub>. The former system is found to have an atomically abrupt interface, with no significant density of interface states. For CoO, however, an interfacial electronic spectrum, different from that of either the substrate or the overlayer, is found. The spatial extent and possible origin of those interfacial states is discussed.

been widely studied, and microscopic pictures of both their interfacial geometry and electronic states have been developed.<sup>[1,2]</sup> There has also been a great deal of experimental, and some theoretical, work on the interfaces between metal oxides and metal overlayers.<sup>[3]</sup> The broad principles of oxide–metal interface formation are fairly well understood (*e.g.*, parameters such as relative cation oxygen affinities),<sup>[4,5]</sup> although a great deal remains to be learned about the behavior of specific oxide–metal interfaces.

The properties of the interfaces between two different metal oxides have become extremely important as high-temperature superconductors, colossal magnetoresistance materials, ferroelectrics, etc. are increasingly being incorporated into solid-

state devices, and as the dimensions of devices shrink. A striking example of oxide–oxide interfacial properties is the recent observation that the interface between SrTiO<sub>3</sub> and LaAlO<sub>3</sub>, both of which are wide-bandgap insulators, is conducting, and also superconducting.<sup>[6–8]</sup> It is of great importance to address the changes in electronic structure that can occur at oxide–oxide interfaces. Some of the earliest work was by González-Elipé and co-workers; they studied both TiO<sub>2</sub><sup>[9–11]</sup> and tin oxides<sup>[12–14]</sup> deposited onto amorphous SiO<sub>2</sub> and single-crystal MgO (100) surfaces by using uv-visible spectroscopy, ion scattering spectroscopy (ISS), x-ray and ultraviolet photoelectron spectroscopies (XPS and UPS), Auger spectroscopy and electron-energy-loss spectroscopy (EELS). For TiO<sub>2</sub>–SiO<sub>2</sub> and TiO<sub>2</sub>–MgO interfaces, the authors were able to monitor the narrowing of the energy gap across the interface and identified the formation of Ti–O–Si and Ti–O–Mg bonds, with an attendant decrease in the positive charge of the Ti ions at the interface. Similar techniques have been used by other groups on other oxide systems,<sup>[15–25]</sup> but detailed determinations of the electronic density-of-states at an oxide–oxide interface were not obtained.

The most important electronic states of interfaces in device applications are those of the valence and conduction bands near E<sub>F</sub>, since those states transfer charge along and across interfaces. Spatially resolved EELS, which probes conduction bands near E<sub>F</sub>, has been used to study the electronic structure changes at perovskite oxide heterointerfaces.<sup>[26–28]</sup> UPS is another sensitive tool for determining the electronic density-of-states in that energy region, primarily the valence bands near E<sub>F</sub>.<sup>[3]</sup> We have therefore examined ways in which UPS can be used to measure

## 1. Introduction

The electronic properties of solid–solid interfaces are of critical importance for a wide range of technological and device applications. The interfaces of semiconductors such as Si and GaAs with many metals and some oxides (*e.g.*, SiO<sub>x</sub>/SiO<sub>2</sub> on Si) have

[\*] Prof. V. Henrich

Center for Research on Interface Structures and Phenomena  
Department of Applied Physics, Yale University  
New Haven, CT 06520 (USA)  
E-mail: victor.henrich@yale.edu

Dr. H.-Q. Wang

Center for Research on Interface Structures and Phenomena  
Department of Applied Physics, Yale University  
New Haven, CT 06520 (USA)

Prof. E. Altman

Center for Research on Interface Structures and Phenomena  
Department of Chemical Engineering, Yale University  
New Haven, CT 06520 (USA)

Prof. C. Broadbridge

Center for Research on Interface Structures and Phenomena  
Department of Physics, Southern Connecticut State University  
New Haven, CT 06515 (USA)

Dr. Y. Zhu

Center for Research on Interface Structures and Phenomena  
Center for Functional Nanomaterials  
Brookhaven National Laboratory  
Upton, NY 11973 (USA)

DOI: 10.1002/adma.200903759

interfacial densities-of-states. We have developed a new method of determining interface electronic structure that involves growing heteroepitaxial layers of one metal oxide on another, one monolayer (ML) at a time. The UPS spectra for those samples are then compared to calculated spectra based on specific models of the oxide–oxide interface. Since the escape depth of the photoemitted electrons in UPS is several monolayers, the spectra for ultrathin overlayers contain information on both the overlayer and the substrate, as well as any electronic states that may exist at the interface. We have successfully applied this technique to NiO–Fe<sub>3</sub>O<sub>4</sub> and CoO–Fe<sub>3</sub>O<sub>4</sub> and have determined the electronic structure near E<sub>F</sub> at their interfaces.

## 2. Structure and Properties of Fe<sub>3</sub>O<sub>4</sub>, CoO and NiO

The systems NiO–Fe<sub>3</sub>O<sub>4</sub> and CoO–Fe<sub>3</sub>O<sub>4</sub> were chosen for several reasons. They are of current interest in novel device applications, since Fe<sub>3</sub>O<sub>4</sub> (magnetite) is a conducting ferrimagnet that some calculations predict should be half-metallic,<sup>[29]</sup> and NiO and CoO are antiferromagnetic insulators; all of these oxides are of potential interest for use in spintronics devices.<sup>[30]</sup> Also, previous work showed that, at least for NiO–Fe<sub>3</sub>O<sub>4</sub>, high quality heteroepitaxial structures could be grown fairly easily.<sup>[31]</sup> Although Fe<sub>3</sub>O<sub>4</sub> has the (inverse) spinel structure, while NiO and CoO have the rocksalt structure, both structures have the same cubic close-packed oxygen sublattice; the two structures differ only in the placement of the cations within that sublattice (see **Figure 1a**). For the (100) planes, which are the ones studied here, the lattice mismatch between the oxygen sublattices is only 0.55% for NiO–Fe<sub>3</sub>O<sub>4</sub>, and 1.45% for CoO–Fe<sub>3</sub>O<sub>4</sub>.

In addition, the valence and conduction band electronic densities-of-states of the three oxides are sufficiently different that they can be easily distinguished in UPS spectra.<sup>[3,32,33]</sup> Lastly, the cations involved (Fe, Ni, and Co) all have comparable oxygen affinities.<sup>[34]</sup> Thus, when one oxide is grown on another, there is no strong competition of one cation for the oxygen in the other oxide. The interfaces are thus fairly inert chemically, which reduces the tendency for cation intermixing at the interface.

## 3. Experimental Approach

The growth and characterization experiments were conducted in a multiple-chamber ultrahigh vacuum (UHV) system consisting of an oxide molecular beam epitaxy (MBE) chamber connected to an analysis chamber. The MBE chamber contained both high temperature effusion cells (used for Ni and Co deposition) and an electron-beam evaporator (for Fe deposition); it is also equipped with reflection high energy electron diffraction (RHEED) to monitor growth. The analysis chamber is equipped with UPS, XPS and Auger spectroscopies, and low energy electron diffraction (LEED). It also contains an effusion cell that can be used to deposit either Ni or Co onto the substrate *in situ* while the sample was positioned in front of the double-pass CMA electron spectrometer (see Section 6 below.) Samples could be transferred between the chambers under UHV. For each series of thin film growths, the sample is transferred to precisely the same position in front of the CMA to collect the UPS data.

Calibration of the evaporation rates of the e-beam evaporator and the effusion cells in the MBE chamber was performed

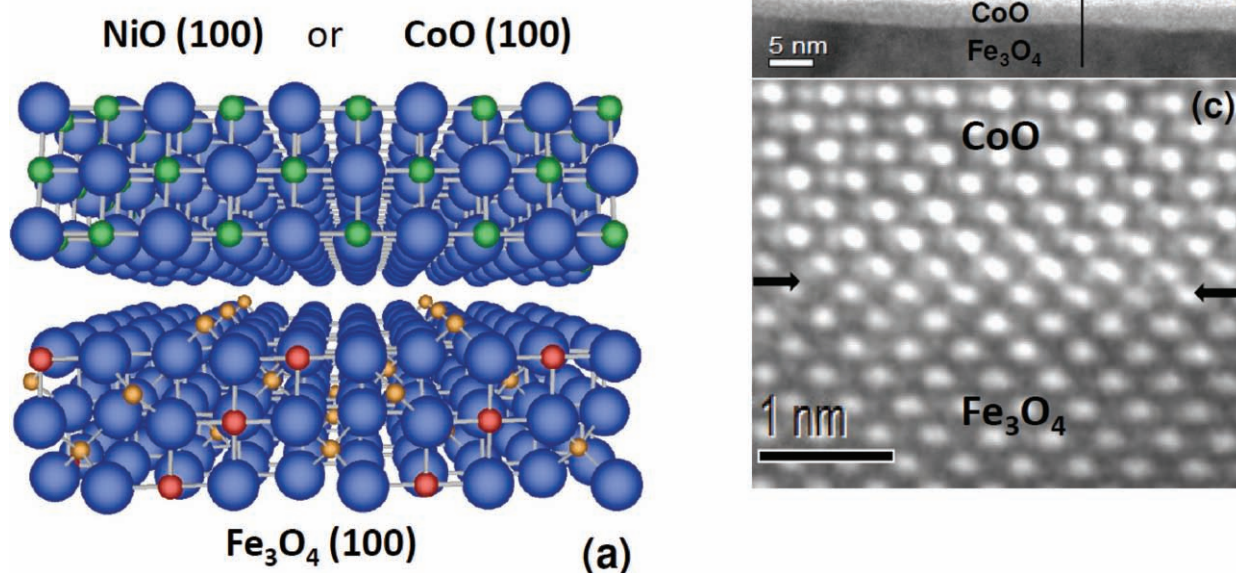


**Figure 1.** a) Model of the interface between Fe<sub>3</sub>O<sub>4</sub> (100) and either NiO or CoO (100). The blue spheres are O anions; green are Ni or Co cations; red are Fe cations in octahedral sites; and orange are Fe cations in tetrahedral sites. b) TEM image of a CoO film grown on Fe<sub>3</sub>O<sub>4</sub> (100), viewed along a [001] zone axis (the arrow indicates the growth direction). c) Nearly atomically sharp interface (as indicated by the two arrows) between the CoO film and the Fe<sub>3</sub>O<sub>4</sub> (100) substrate.

using a quartz crystal thickness monitor located at the sample position. The deposition rate of the effusion cell in the analysis chamber was calibrated by comparing XPS and Auger spectra for various overlayer thickness with those grown in the MBE chamber. The  $\text{Fe}_3\text{O}_4$  (100) substrates used were 40 nm thick films grown heteroepitaxially on single-crystal  $\text{MgO}$  (100) plates.<sup>[32]</sup> The surface structure observed was the  $\sqrt{2} \times \sqrt{2}$  R45°, which is the reconstruction usually observed on the stoichiometric, charge neutral surface.<sup>[35]</sup>

Since  $\text{Fe}_3\text{O}_4$  is not the maximal valency oxide of Fe, care must be taken when growing another oxide on  $\text{Fe}_3\text{O}_4$  in order to avoid oxidizing its surface to  $\text{Fe}_2\text{O}_3$ . Here the first monolayer of NiO or CoO was grown by depositing in UHV just enough Ni or Co to be oxidized to one monolayer of NiO or CoO. The surface was then exposed to just enough  $\text{O}_2$  to oxidize the metal. The second through fifth monolayers were grown one at a time in the same way. Beyond the fifth layer, the metal was simply deposited in an  $\text{O}_2$  ambient. In all cases, an overlayer at least 2 nm thick was grown (thick film) to use as a standard for the overlayer oxide, when there was no contribution from the substrate to the UPS spectra.

UPS spectra were taken using the 40.8 eV He II line from a helium discharge lamp. The photoemitted electrons were analyzed using a PHI double-pass CMA. All UPS spectra were corrected for the presence of other spectral lines in the gas discharge.

Cross-sectional high resolution transmission electron microscopy (HRTEM) images, recorded on a 300 kV JEOL 3000F with a point resolution of 0.165 nm, were used to observe directly the geometric quality of the oxide–oxide interfaces. Figure 1b shows TEM images on one of the CoO (100) films grown on  $\text{Fe}_3\text{O}_4$  (100), across an 18 nm field of view. The atomic imaging of the interface, Figure 1c, shows the excellent registry of the atomic structure from the substrate to the film of CoO, without visible dislocations. It indicates the coherent nature of the interface, *i.e.*, the in-plane lattice parameter of the CoO film is equal to that of the  $\text{Fe}_3\text{O}_4$  substrate. Thus the film is commensurate with a strain of 1.45%, compared to its bulk structure. Although this interface appears to be atomically sharp, it does not necessarily imply electronic abruptness, as we will discuss in Section 5 below from UPS measurements.

#### 4. Theoretical Models

A model of the oxide–oxide interface is necessary in order to interpret the UPS spectra obtained from samples with different overlayer thicknesses. The mean-free-path,  $\lambda$ , of He II photoelectrons (about 5–10 Å) is large enough that UPS spectra will sample several ML into the sample. For thin overlayers, the measured spectra will thus consist of a superposition of emission from the substrate, any interfacial states that may be present, and the overlayer, with each weighted by electron escape depths. We begin by comparing the measured UPS spectra to a model of the spectra that would be expected if they consisted simply of a superposition of the bulk spectrum for the substrate and that of the overlayer (thick film), *without* any interface states present. Assuming layer-by-layer growth, the

spectral intensity  $I$  as a function of thin film thickness  $d$  is then calculated from:<sup>[36]</sup>

$$I(d) = I_O^{\text{Substrate}} \exp(-d/\lambda) + I_O^{\text{Film}} [1 - \exp(-d/\lambda)] \quad (1)$$

The experimental clean substrate spectrum and the thick film overlayer spectrum are taken as the respective bulk spectra,  $I_O^{\text{Substrate}}$  and  $I_O^{\text{Film}}$ ; this is necessary because the angular dependence of electron emission from single-crystal samples causes UPS spectra to change slightly with the position of the sample in front of the (semi-angle resolved) electron spectrometer, and because the contribution of interface states to the UPS spectra may be small. That is the reason that the sample is positioned in precisely the same position in front of the spectrometer after each deposition. Differences between the measured and model spectra should thus result from the interfacial electronic structure.

The value for the photoelectron mean-free-path,  $\lambda$ , is determined from the best fit to the attenuation of the overlayer cation features in the UPS spectra as a function of overlayer thickness from Equation (1). The overlayer thickness,  $d$ , is determined from the deposition rates calibrated using the thickness monitor.

For NiO– $\text{Fe}_3\text{O}_4$ , the experimental UPS data were found to fit Equation (1) extremely well, indicating effectively no interfacial electronic states; see Section 5 below. However, for CoO– $\text{Fe}_3\text{O}_4$ , the experimental spectra differed significantly from the model given by Equation (1), indicating the presence of interface states.

When interface states are present, Equation (1) can be modified to:<sup>[36]</sup>

$$I'(d) = I_O^{\text{Substrate}} \exp[-(d + d_{is})/\lambda] + I_O^{\text{Film}} \{1 - \exp[-(d - d_{io})/\lambda]\} + I_O^{\text{Interface}} [1 - \exp(-d_i/\lambda)] \exp[-(d - d_{io})/\lambda] \quad (2)$$

In this model, a thickness  $d_{is}$  of the substrate becomes part of the interfacial layer, as does a thickness  $d_{io}$  of the overlayer; so the total thickness of the interfacial layer is  $(d_{is} + d_{io})$ .  $I_O^{\text{Interface}}$  is the spectral intensity for the interface layer, assuming that one had a semi-infinite slab having the interface electronic structure.  $d$  is the total thickness of the overlayer deposited.

#### 5. Data Analysis

This section describes the basic analysis of the data for NiO– $\text{Fe}_3\text{O}_4$  and CoO– $\text{Fe}_3\text{O}_4$ . Various issues may arise in the course of the analyses, and some of those are discussed in Section 6 below.

**NiO– $\text{Fe}_3\text{O}_4$ :** When NiO (100) overlayers were deposited onto  $\text{Fe}_3\text{O}_4$  (100) substrates, the UPS spectra were extremely well described by Equation (1), which assumes that *no interfacial electronic states* are present.<sup>[33]</sup> This is shown in **Figure 2a** for one experimental run. Figure 2(a,i) shows the experimental UPS spectra, after correction for additional lines in the He II lamp and removal of a Li background<sup>[37]</sup> of inelastically scattered electrons, for the clean  $\text{Fe}_3\text{O}_4$  (100) substrate, and 1, 2, 3 and 20 (thick film) ML of NiO (100). Using the substrate and 20 ML NiO spectra as  $I_O^{\text{Substrate}}$  and  $I_O^{\text{Film}}$ , respectively, and Equation (1) (*i.e.*, assuming no interface states), the calculated UPS spectra

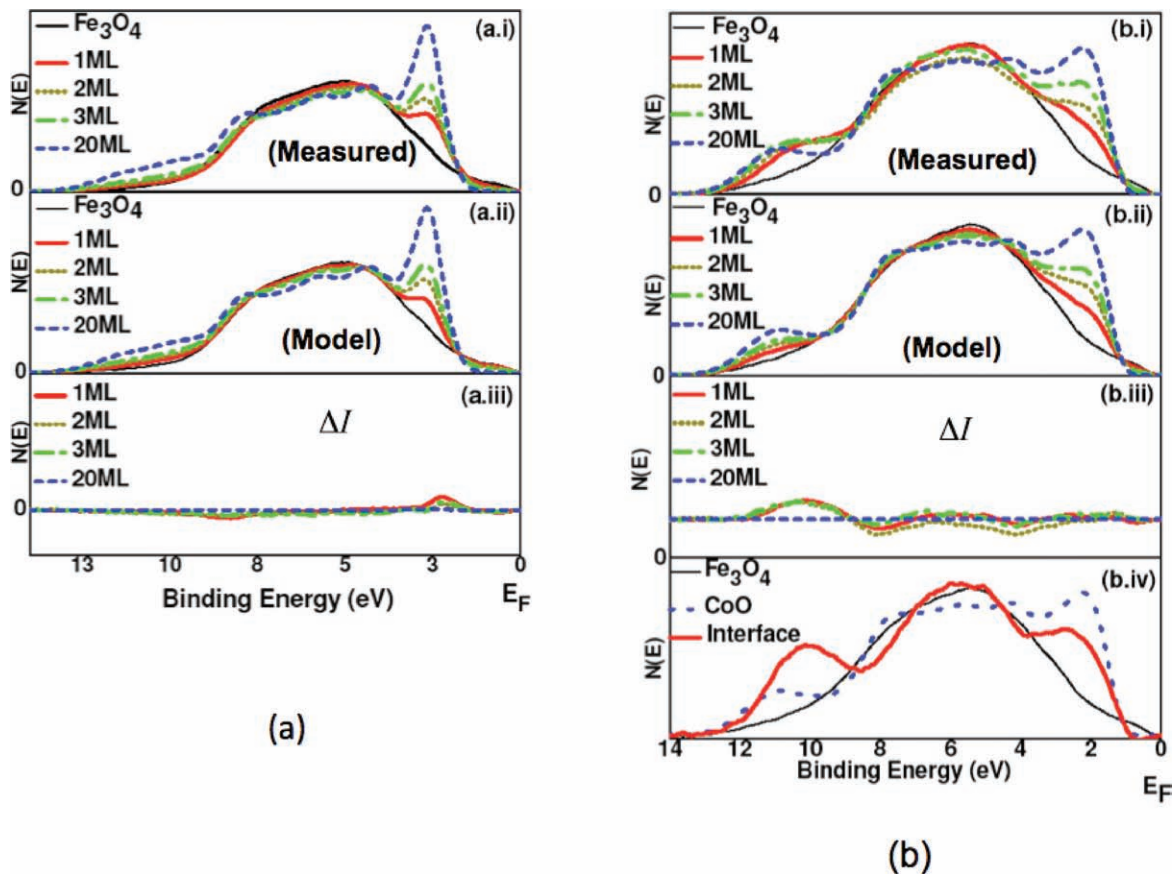


**Figure 2.** a) Experimental (a,i) and theoretical (a,ii) UPS spectra of NiO films grown on  $\text{Fe}_3\text{O}_4$ . An inelastic Li background (see Ref.[37]) has been subtracted from the experimental spectra. (a,iii) Difference spectra taken by subtraction model spectra from measured spectra. b) Experimental (b,i) and theoretical (b,ii) UPS spectra of CoO films grown on  $\text{Fe}_3\text{O}_4$ . An inelastic Li background has been subtracted from the experimental spectra. (b,iii) Difference spectra taken by subtraction model spectra from measured spectra. (b,iv) Comparison of the spectra for the  $\text{Fe}_3\text{O}_4$  substrate, the thickest CoO film (both from Figure 2b) and the interfacial electronic state. Adapted from Ref.[38].

for those overlayer thicknesses are presented in Figure 2(a,ii). The similarity of the two sets of spectra is shown quantitatively in Figure 2(a,iii), which plots the measured spectra minus the model spectra for each of the four NiO thickness in Figures 2a,i and 2a,ii. There are small differences between the two, particularly for the 1 ML spectrum, but overall the agreement is excellent.

At this point, it is necessary to consider *quantitatively* what one would expect to see in UPS spectra if interface states were present. To do this, we took the experimental data from Figure 2(a), assuming that no interface states were present there, and added an arbitrary “interface” contribution to the spectra; this model is shown in Figure 3. Figure 3a re-plots the experimental data from Figure 2a,i, and then adds a spectrum consisting of two Gaussians, plotted as the dark red curve. We assume that this Gaussian spectrum is the electronic density-of-states of an interface layer. The energy locations of the Gaussians were chosen so that one of them ( $\sim 7$  eV) could be easily distinguished from any features of the  $\text{Fe}_3\text{O}_4$  or NiO spectra, while the other ( $\sim 3.2$  eV) lies under the main NiO feature; the latter was chosen to see how easy it would be to identify such a feature as an interface state. The amplitudes of the Gaussians in Figure 3a are comparable to features in the  $\text{Fe}_3\text{O}_4$  and NiO spectra. We thus assume

that the interface spectrum plotted is what one would see for a semi-infinite slab of an imaginary material having the interface electronic structure.

Equation (2) was then used to compute what the UPS spectra would look like if that interface were present. In Figure 3, the interfacial layer is assumed to be 1 ML thick, and the amplitude of the interface contribution to the UPS spectra is scaled down accordingly. The model UPS spectra are plotted in Figure 3b for a total overlayer thickness of 3 ML, both without (thin solid black curve) and with (pink dashed curve) interface states present. These spectra can be directly compared with the experimental data in Figure 2a,i. The changes in the spectra caused by the presence of interface states in Figure 3b are at least an order of magnitude larger than any differences observed in Figure 2a, leading to the conclusion that there are essentially no interface states in the NiO– $\text{Fe}_3\text{O}_4$  system, and that the interface is atomically abrupt both structurally and electronically.

Figure 3 shows another aspect of our approach that is crucial to the detailed analysis of experimental data. In Figure 3b, three arrows identify features in the UPS spectra that are characteristic of the substrate  $\text{Fe}_3\text{O}_4$  (the shoulder at 0.66 eV that is due to the  $\text{Fe}^{2+}$  3d<sup>6</sup> cations in magnetite) and the NiO overlayer (the Ni 3d peak at 2.66 eV), and in the difference spectra

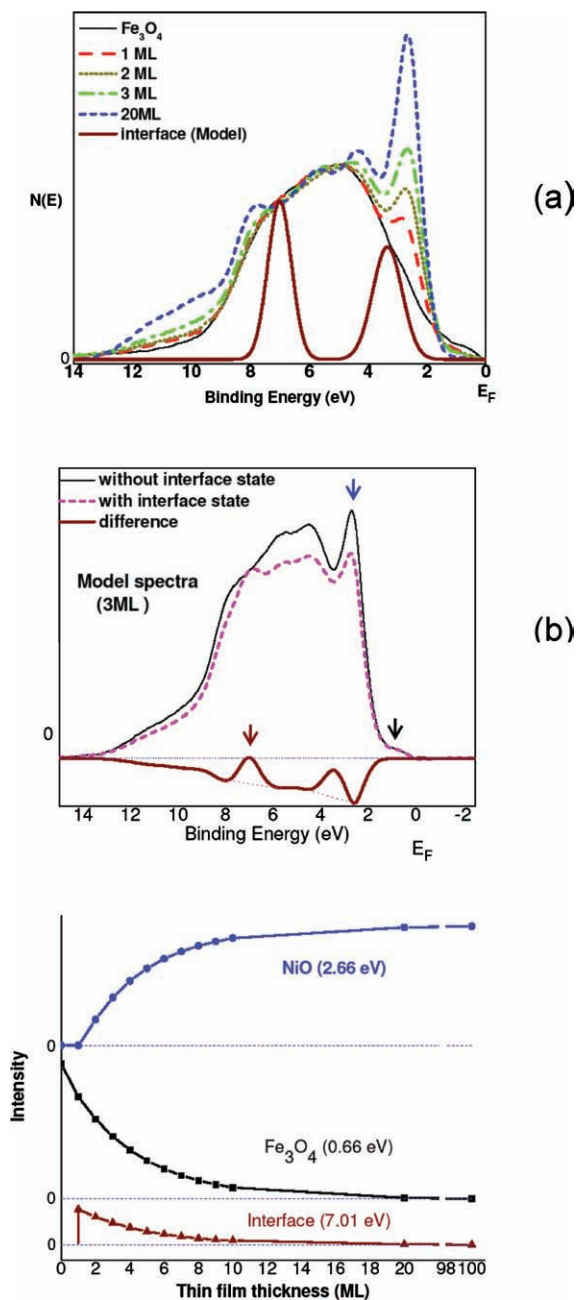


**Figure 3.** a) Experimental UPS spectra for NiO films grown on Fe<sub>3</sub>O<sub>4</sub>, and a hypothetical interface electronic state spectrum; see text for details. b) Model UPS spectra for a 3 ML NiO film on Fe<sub>3</sub>O<sub>4</sub>, based on the data in Figure 3a, with (red curve) and without (black curve) the interface state. The purple curve is the difference spectrum between the two. (See text for discussion of the arrows.) c) Dependence of the amplitude of the substrate, overlayer and interface features in the UPS spectra as a function of overlayer film thickness.

for the interface state (the Gaussian at 7.01 eV). Figure 3c then plots how the calculated amplitudes of those features change as a function of total NiO overlayer thickness. As mentioned above, we have assumed here an interface layer 1 ML thick. No interface features are present on the clean substrate, of course; however, they appear when the first monolayer of NiO is depos-

ited, i.e., as the interface is formed. In our model, this layer is entirely interface, so no NiO features are present for 1 ML. The second ML of NiO goes down as NiO, however, on top of the 1 ML of interface. Thus the contributions of the various layers of the sample to the UPS should be identifiable by the thickness dependence of their amplitudes. This is part of the detailed analysis that is necessary in order to fully determine the electronic density-of-states at the interface; see Ref.<sup>[36]</sup> for specifics.

**CoO–Fe<sub>3</sub>O<sub>4</sub>:** Although CoO and NiO are identical to each other structurally and closely related electronically,<sup>[3]</sup> their interfaces with Fe<sub>3</sub>O<sub>4</sub> are distinctly different.<sup>[32,38]</sup> Figures 2b,i–iii show the results of measurements on the CoO–Fe<sub>3</sub>O<sub>4</sub> interface similar to those for NiO–Fe<sub>3</sub>O<sub>4</sub> in Figure 2a. The measured UPS spectra for the clean Fe<sub>3</sub>O<sub>4</sub> (100) substrate, and 1, 2, 3 and 20 ML of CoO (100), are shown in Figure 2b,i. Figure 2b,ii gives the model spectra from Equation (1) (i.e., assuming no interface states), using the substrate and 20 ML CoO spectra as  $I_O^{Substrate}$  and  $I_O^{Film}$ , respectively. While the two sets of spectra are quite similar, there are noticeable differences that are much larger than those for NiO–Fe<sub>3</sub>O<sub>4</sub>. This can be seen in the difference spectra in Figure 2b,iii. It is thus necessary to use Equation (2) to model the CoO–Fe<sub>3</sub>O<sub>4</sub> UPS spectra.

That the differences between the experimental and model spectra are indeed due to electronic states localized near the interface can be shown qualitatively simply by taking sequential differences between the experimental spectra (not shown).<sup>[36]</sup> The clean Fe<sub>3</sub>O<sub>4</sub> spectrum is subtracted from the 1 ML spectrum; the 1 ML spectrum is subtracted from the 2 ML spectrum; the 2 ML is subtracted from the 3 ML; and so forth. These sequential difference spectra give, to first order, the electronic structure of each monolayer of CoO deposited. It is found that the “1 ML minus the substrate” spectrum is different from either the Fe<sub>3</sub>O<sub>4</sub> or thick film CoO spectra, but that, from the “2 ML minus 1 ML” spectrum on to thicker overlayers, the sequential differences look very much like the CoO spectrum. This indicates that the “different” electronic structure involves only the first ML of CoO and does not spread into the thicker CoO layers.

To accurately extract the interfacial density-of-states from the experimental UPS spectra, the data must be compared to a more detailed model of the interface than is given by Equation (2). The number of monolayers of Fe<sub>3</sub>O<sub>4</sub> and of CoO that are involved in formation of the interfacial layer must be assumed, and the data then analyzed using a modification of Equation (2). For CoO–Fe<sub>3</sub>O<sub>4</sub>, several such models were employed; the details of the process are given in Ref.<sup>[36]</sup>. For each interface model, a set of UPS spectra was calculated. The most accurate way to compare the various models to the experimental data turned out to be *via* the sequential differences discussed above.

For CoO–Fe<sub>3</sub>O<sub>4</sub>, the best fit of theory to experiment is for an interfacial layer that involves one ML of CoO and the first ML of Fe<sub>3</sub>O<sub>4</sub> from the substrate. This model gives a significantly better fit to the data than does any other. Using the modification of Equation (2) appropriate for that model, the electronic density-of-states within this interfacial layer can be determined; it is given as the thick red curve in Figure 2(b,iv), where it is compared to both the substrate (thin black curve) and overlayer (dashed blue curve) spectra. While features of both the Fe and Co

oxides can be seen in the interfacial density-of-states, there is clearly a distinctly different electronic structure confined to the two atomic layers at the CoO–Fe<sub>3</sub>O<sub>4</sub> interface.

One of the reasons that the CoO–Fe<sub>3</sub>O<sub>4</sub> interface is not as sharp electronically as that of NiO–Fe<sub>3</sub>O<sub>4</sub> could be due to the greater lattice mismatch (1.45%) in the former case. The strains caused by lattice mismatch may be small enough to allow epitaxial growth for both systems, but it may still cause the bonding configuration (bond length, bond angle, etc.) in the interface to be different than those in the substrate and the overlayer, thus generating distinct interfacial electronic states. Another reason could be the difference in *d*-orbital configuration of Co<sup>2+</sup> (3d<sup>7</sup>) and Ni<sup>2+</sup> (3d<sup>8</sup>).<sup>[39,40]</sup> The t<sub>2g</sub> band is filled for Ni<sup>2+</sup>, but for Co<sup>2+</sup> it is missing one electron. When very thin CoO films are deposited onto the Fe<sub>3</sub>O<sub>4</sub> substrate, charge transfer may occur by moving an electron from the t<sub>2g</sub> band of Fe<sup>2+</sup> to fully fill that of Co<sup>2+</sup>. The resulting 3d<sup>5</sup> configuration for the Fe<sup>3+</sup> cation is generally the lowest energy state in iron compounds. Thus Fe<sup>2+</sup> → Co<sup>2+</sup> charge transfer might also be the origin of the observed interface states.

## 6. Additional Considerations

The above procedure is a relatively straightforward way to determine the electronic density-of-states near E<sub>F</sub> at a solid–solid interface. However, care must be taken in applying the technique. Already mentioned above is the fact that when UPS spectra from single-crystal samples are measured by an angle-resolved electron spectrometer, or by a semi-angle-resolved spectrometer such as the CMA used in this work, the spectra are sensitive to the positioning of the sample in front of the spectrometer. Thus great care must be exercised each time the sample is transferred from the growth chamber to the analysis chamber and repositioned at the focal point of the electron spectrometer. If possible, it would be desirable to deposit the overlayer while the sample is positioned at the spectrometer focal point, without moving the sample during the depositions or UPS measurements. We have used both methods in our experiments on Ni–Fe<sub>3</sub>O<sub>4</sub> and CoO–Fe<sub>3</sub>O<sub>4</sub>.

Another effect that can cause serious problems for the interpretation of UPS spectra is sample charging. For the systems studied here, the substrate is conducting, so surface charging was not a major problem. However, both NiO and CoO are insulators when stoichiometric, so the overlayer films could exhibit some surface charging when sufficiently thick. This should not be a problem for the first few monolayers, since charge can tunnel through the thin film, but a thick overlayer spectrum is also required for use as I<sub>O</sub><sup>Film</sup>. The first-order effect of surface charging on UPS spectra is to shift the spectra to higher apparent binding energy. If one takes the difference between two identical spectra that are slightly shifted relative to each other in energy, the result is a difference spectrum that is very nearly the first derivative with respect to energy of the actual spectrum;<sup>[41]</sup> if the spectral features are sharp, the amplitude of the difference can be quite large for a very small shift in energy. We observed this in some of our data, and it was thus necessary to shift some spectra slightly (tens of meV) in order to eliminate this artifact.

As mentioned above, the cations in the oxide–oxide systems studied here all have comparable oxygen affinities,<sup>[34]</sup> resulting in interfaces that are fairly inert chemically. If the cation oxygen affinities are very different in the two oxides, the interfaces can be quite complex. An example where the interface would be very chemically reactive would be depositing Ti or Mg (which have very high oxygen affinities) onto any transition-metal oxide, since the Ti or Mg would tend to reduce the surface of the substrate. In such a case, it could be difficult to model the stoichiometry of the interface for comparison with experimental data.

## 7. Conclusions

We have utilized the finite escape depth of the photoemitted electrons in UPS to examine the electronic density-of-states at the interfaces between two dissimilar metal oxides. By growing heteroepitaxial ultrathin films of one oxide on a single-crystal substrate of another, a single monolayer at a time, we have shown that the electron density-of-states near E<sub>F</sub> at the interface can be separated from the densities-of-states of the substrate and overlayer oxides. Experimental UPS spectra of the valence and conduction bands are compared with calculated spectra derived from specific models for the interfacial structure. For the NiO–Fe<sub>3</sub>O<sub>4</sub> system, where the lattice mismatch is only 0.55%, no detectable density of interfacial electronic states is observed; the interface appears to be electronically atomically abrupt (as it is structurally). For CoO–Fe<sub>3</sub>O<sub>4</sub>, however, a distinct spectrum of electronic states is found to exist at the interface, which includes the outermost atomic layer of the substrate and the first atomic layer of the overlayer oxide. These states could arise from effects of lattice strain, or from electron transfer across the interface, resulting in more stable cation electron configurations. This approach to determining interfacial electronic structure should be applicable to a wide range of solid–solid systems.

## Acknowledgements

This work was partially supported by the National Science Foundation under Grant No. MRSEC DMR-0520495.

Received: November 4, 2010  
Published online: April 13, 2010

- [1] J. W. Reiner, K. F. Garrity, F. J. Walker, S. Ismail-Beigi and C. H. Ahn, *Phys. Rev. Lett.* **2008**, *101*, 105503.
- [2] Y. Segal, J. W. Reiner, A. M. Kolpak, Z. Zhang, S. Ismail-Beigi, C. H. Ahn and F. J. Walker, *Phys. Rev. Lett.* **2009**, *102*, 116101.
- [3] V. E. Henrich, P. A. Cox, *The Surface Science of Metal Oxides*, Cambridge University Press, Cambridge, **1994**.
- [4] V. E. Henrich, *Mat. Res. Soc. Symp. Proc.* **1995**, *357*, 67.
- [5] M. W. Finnis, *J. Phys.: Condens. Matter* **1996**, *8*, 5811.
- [6] A. Ohtomo, H. Y. Hwang, *Nature* **2004**, *427*, 423.
- [7] N. Reyren, S. Thiel, A. D. Caviglia, L. Fitting Kourkoutis, G. Hammerl, C. Richter, C. W. Schneider, T. Kopp, A.-S. Rüetschi, D. Jaccard, M. Gabay, D. A. Muller, J.-M. Triscone, J. Mannhart, *Science* **2007**, *317*, 1196.

- [8] J. W. Reiner, F. J. Walker, C. H. Ahn, *Science* **2009**, 323, 1018.
- [9] G. Lassaletta, A. Fernández, J. P. Espinós, A. R. González-Elipe, *J. Phys. Chem.* **1995**, 99, 1484.
- [10] J. A. Mejías, V. M. Jiménez, G. Lassaletta, A. Fernández, J. P. Espinós, A. R. González-Elipe, *J. Phys. Chem.* **1996**, 100, 16255.
- [11] V. M. Jiménez, G. Lassaletta, A. Fernández, J. P. Espinós, A. R. González-Elipe, *Surf. Interface Anal.* **1997**, 25, 292.
- [12] V. Jiménez, A. Fernández, J. P. Espinós, A. R. González-Elipe, *Surf. Sci.* **1996**, 350, 123.
- [13] V. Jiménez, J. A. Mejías, J. P. Espinós, A. R. González-Elipe, *Surf. Sci.* **1996**, 366, 545.
- [14] V. Jiménez, J. P. Espinós, A. R. González-Elipe, *Surf. Sci.* **1996**, 366, 556.
- [15] R. J. Lad, *Surf. Rev. Lett.* **1995**, 2, 109.
- [16] S. Imaduddin, A. M. Davidson, R. J. Lad, *Mat. Res. Soc. Symp. Proc.* **1995**, 357, 177.
- [17] Y. Yu, R. J. Lad, *Mat. Res. Soc. Symp. Proc.* **1995**, 357, 47.
- [18] S. Imaduddin, R. J. Lad, *Mat. Res. Soc. Symp. Proc.* **1996**, 401, 507.
- [19] S. C. Moulzolf, Y. Yu, D. J. Frankel, R. J. Lad, *J. Vac. Sci. Technol. A* **1997**, 15, 1211.
- [20] J. M. Sanz, G. T. Tyuliev, *Surf. Sci.* **1996**, 367, 196.
- [21] Q. Guo, C. Xu, D. E. Goodman, *Langmuir* **1998**, 14, 1371.
- [22] C. Xu, W. S. Oh, Q. Guo, D. W. Goodman, *J. Vac. Sci. Technol. A* **1996**, 14, 1395.
- [23] T. Fujii, D. Alders, F. C. Voogt, T. Hibma, B. T. Thole, G. A Sawatzky, *Surf. Sci.* **1996**, 366, 579.
- [24] Y. Shao, W. Chen, E. Wold, J. Paul, *Langmuir* **1994**, 10, 178.
- [25] M. L. Burke, D. W. Goodman, *Surf. Sci.* **1994**, 311, 17.
- [26] A. Ohtomo, D. A. Muller, J. L. Grazul, H. Y. Hwang, *Nature* **2002**, 419, 378.
- [27] N. Nakagawa, H. Y. Hwang, D. A. Muller, *Nat. Mater.* **2006**, 5, 204.
- [28] D. A. Muller, L. Fitting Kourkoutis, M. Murfitt, J. H. Song, H. Y. Hwang, J. Silcox, N. Dellby, O. L. Krivanek, *Science* **2008**, 319, 1073.
- [29] Z. Szotek, W. M. Temmerman, D. Ködderitzsch, A. Svane, L. Petit, H. Winter, *Phys. Rev. B* **2006**, 74, 174431.
- [30] S. A. Wolf, D. D. Awschalom, R. A. Buhrman, J. M. Daughton, S. von Molnár, M. L. Roukes, A. Y. Chtchelkanova, D. M. Treger, *Science* **2001**, 294, 1488.
- [31] D. M. Lind, S. D. Berry, G. Chern, H. Mathias, L. R. Testardi, *Phys. Rev. B* **1992**, 45, 1838.
- [32] H.-Q. Wang, E. I. Altman, V. E. Henrich, *Phys. Rev. B* **2008**, 77, 085313.
- [33] H.-Q. Wang, W. Gao, E. I. Altman, V. E. Henrich, *J. Vac. Sci. Technol. A* **2004**, 22, 1675.
- [34] T. B. Reed, *Free Energy of Formation of Binary Compounds*, MIT Press, Cambridge, **1971**.
- [35] H.-Q. Wang, E. I. Altman, V. E. Henrich, *Phys. Rev. B* **2006**, 73, 235418-7.
- [36] H. Q. Wang, *Structure of the Fe<sub>3</sub>O<sub>4</sub> (100) Surface and Its Interfaces with NiO (100) and CoO (100) Overlayers*, Ph.D. thesis, Yale University, **2007**.
- [37] X. Li, Z. Zhang, V. E. Henrich, *J. Electron Spectros.* **1993**, 63, 253.
- [38] H.-Q. Wang, E. I. Altman, V. E. Henrich, *Appl. Phys. Lett.* **2008**, 92, 012118.
- [39] M. Hassel, H. Kuhlenbeck, H.-J. Freund, S. Shi, A. Freitag, V. Staemmler, S. Liitkehoff, M. Neumann, *Chem. Phys. Lett.* **1995**, 240, 205.
- [40] H. Takahashi, F. Munakata, M. Yamahaka, *J. Phys. Condens. Matter* **1995**, 7, 1583.
- [41] V. E. Henrich, *Surf. Sci.* **1993**, 284, 200.